ACS APPLIED MATERIALS & INTERFACES

Research Article

www.acsami.org

Polymer Brush Surfaces Showing Superhydrophobicity and Air-Bubble Repellency in a Variety of Organic Liquids

Gary J. Dunderdale, Matt W. England, Chihiro Urata, and Atsushi Hozumi*

National Institute of Advanced Industrial Science and Technology (AIST), 2266-98, Anagahora, Shimoshidami, Moriyama, Nagoya 463-8560, Japan

Supporting Information

ABSTRACT: Silicon (Si) substrates were modified with polyalkyl methacrylate brushes having different alkyl chain lengths (C_n, where n = 1, 4, 8, and 18) using ARGET-ATRP at ambient temperature without purging the reaction solution of oxygen. The dynamic hydrophobicity of these polymer brush-covered Si surfaces when submerged in a variety of organic solvents (1-butanol, dichloromethane, toluene, n-hexane) depended markedly on the alkyl chain length and to a lesser extent polymer solubility. Long-chain poly(stearyl methacrylate) brushes (C_n = 18) submerged in toluene showed excellent water-repellant properties, having large advancing/receding contact angles (CAs) of 169°/168° with negligible CA hysteresis (1°). Whereas polymer brushes with short alkyl-chain ($C_n \leq 4$) had significantly worse water drop mobility because of small CAs (as low as 125°/55°) and large CA hysteresis (up to 70°). However, such poor dynamic dewetting behavior of these surfaces was found to significantly improve when water drops impacted onto the surfaces at moderate velocities. Under these conditions, all brush surfaces were able to expel water drops from their surface. In addition, our brush surfaces were also highly repellant toward air bubbles under all conditions, irrespective of C_n or polymer solubility. These excellent surface properties were found to be vastly superior to the performance of conventional perfluoroalkylsilane-derived surfaces.

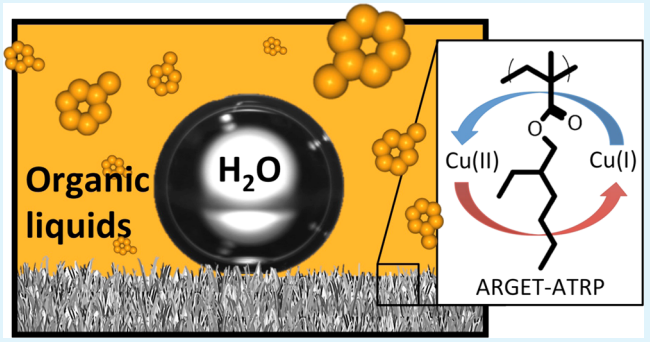

KEYWORDS: *polymer brush, superhydrophobicity, under organic liquids, ARGET-ATRP, air-bubble repellency*

INTRODUCTION

The control of wetting and dewetting on a wide variety of materials is important in everyday life as well as in industrial applications. Adhesion of water drops to surfaces can lead to problems such as corrosion of metals,[1,2] fogging of windshields,[3,4] or calcification of pipes and valves.[5] More seriously, freezing of this contaminant water to form ice has been responsible for aircraft crashes[6] and numerous accidents. To prevent such undesirable adhesion of water droplets to surfaces and overcome these problems, creation of functional surfaces which effectively repel water have been widely investigated.[7] Most studies have particularly focused on creating surfaces which maximize absolute contact angles (CAs) and so decrease the contact area of water drops on the surface. These approaches heavily rely on both surface texturing and perfluorination. However, formation of such textured surfaces can be complicated, requiring many separate processes and clean room techniques, meaning they can be unsuitable for large-scale area functionalization. Precise control of surface roughness is crucial to achieve high transparency, and such fine surface structures can be easily damaged by mechanical abrasion and contaminated by impurities. Furthermore, perfluorinated compounds can be difficult to process and may cause serious damage to human health and the environment.[8,9] Several large international companies have now ceased to use one common precursor to perfluorinated products (perfluorooctanoic acid).[10] We have previously reported that such conventional approaches are not required to create "liquid-repellant" surfaces; instead smooth, transparent, and perfluorinated surfaces can be used. Our approach has particularly focused on minimizing CA hysteresis (difference between advancing and receding CAs) rather than maximizing CAs to improve the motion of probe liquids. On these low-CA-hysteresis surfaces, water and various low-surface tension liquids can move easily without pinning.[11,12]

Besides water repellant surfaces, recent concern has focused on the ability of surfaces to repel various organic liquids when submerged underwater, so-called underwater superoleophobicity. Lui et al.[13] first reported the underwater superoleophobicity of fish scales, which consist of microstructures of calcium phosphate covered with a highly hydrated mucus layer. These fish scales were found to be superoleophobic underwater, with static CAs of 156° (1,2-dichloroethane) and showed excellent oil-repellant properties. They replicated the nano/micro

Received: March 26, 2015
Accepted: May 19, 2015
Published: May 19, 2015

DOI: 10.1021/acsami.5b02634
ACS Appl. Mater. Interfaces 2015, 7, 12220−12229

structure of the fish scales using polyacrylamide gel. This biomimetic surface yielded underwater superoleophobicity, which was better than the original fish scales (static CA = 174° 1,2-dichloroethane). Furthermore, others have also reported similar biomimetic strategies using highly hydrated layers consisting of polymer brushes,[14] polymer gels,[15,16] or polyelectrolyte multilayers.[17,18] We have also previously reported that water-soluble polymer brush surfaces can give excellent underwater oleophobicity and can be prepared on large-scale surfaces by a facile and inexpensive "paint-on" process.[19] Our brush surfaces have the ability to respond to several external stimuli such as solution pH[20] and ionic strength.[21] Thanks to these excellent physicochemical surface properties, the adhesion and mobility of oil drops to the surfaces can be arbitrarily controlled (switched on or off).

With these excellent oil-repellant properties of hydrophilic water-soluble brushes in mind, we wondered if this strategy could be inverted to produce superhydrophobic surfaces when submerged in oils. Such superhydrophobic functional coatings are important for engine and machine parts, oil pipelines, and chemical reactors or storage tanks. To realize such unique surface properties, highly oil-soluble rather than water-soluble polymer brushes are required. Such highly solvated brush surfaces should give large water CAs in oils and effectively repel contaminant water drops.

Polymer brushes are suitable for such functionalization of solid surfaces because their densely packed polymer chains can give enhanced surface properties.[22−25] Of particular importance for real-life surfaces such as machine parts etc. are the excellent lubricating properties of both water-soluble[26,27] and oil-soluble[28,29] polymer brushes, along with their excellent anticorrosion properties.[30,31] Although polymer brushes have been generally grown on silicon (Si) surfaces in the laboratory, they can be grown on a variety of important substrates such as metals, glasses, and plastics through a variety of surface-bound, initiating moieties.[32−35] Polymer brushes have been predominantly prepared using Atom Transfer Radical Polymerization (ATRP).[25] However, ATRP requires oxygen-less reaction conditions and elevated reaction temperatures making it difficult to perform on large-scale surfaces. Thus, a modified ATRP protocol, called Activators (Re)Generated by Electron Transfer (A(R)GET)-ATRP, has attracted increasing attention.[36] Using this protocol, the oxygen sensitivity of the reaction can be effectively removed by the introduction of a reducing agent which converts oxidized copper catalyst back to its reduced state.

In this article, we describe the surface modification of silicon with various hydrophobic polyalkyl methacrylate brushes based on a facile ARGET-ATRP protocol. Particularly, the effect of polyalkyl methacrylate alkyl chain length and molecular structure on hydrophobicity and air-bubble repellency when submerged in a variety of organic liquids is investigated. Such dynamic dewetting behavior of polymer brushes in organic liquids has thus far not been studied, and reports of superhydrophobic surfaces submerged in organic liquids are infrequent.[37] However, as we will show, polymer brushes give superior surface properties compared to conventional perfluoroalkylsilane-derived surfaces.

EXPERIMENTAL SECTION

Materials. (3-Aminopropyl)triethoxysilane (APTES), tin(II) ethylhexanoate, ethanol, toluene, 1-butanol, *n*-hexane, dichloromethane, methyl methacrylate (MMA), *n*-butyl methacrylate (BuMA), *iso*-butyl methacrylate, *tert*-butyl methacrylate, and 2-ethyl-hexyl methacrylate (EHMA) were purchased from Wako Pure Chemical Industries Ltd., Japan, and used as received. Ascorbic acid (AA), stearyl methacrylate (StMA), copper(II) chloride ($CuCl_2$), pentamethyldiethylenetriamine (PMDETA), and α-bromoisobutyryl bromide (BiBB) were purchased from Sigma-Aldrich and used as received. (3,3,3-Trifluoropropyl)-trimethoxysilane (FAS3) and (heptadecafluoro-1,1,2,2,-tetrahydrodecyl)trimethoxysilane (FAS17) were purchased from Gelest Inc.

Preparation of Si Initiator Surfaces. *n*-Type Si (100) wafers used as the polymer brush substrate were cut into small pieces 1−12 cm^2, sonicated in ethanol for 5 min to remove dust and impurities, and then dried in a stream of nitrogen (N_2) gas. Next, these samples were cleaned using UV-ozone treatment for 30 min at 10^3 Pa. They were then placed in a large glass vial placed with a smaller glass vial containing ∼100 μL of APTES, the large vial sealed using a screw top, and then heated at 100 °C for 60 min. This procedure functionalized the silicon surface with APTES via a condensation reaction of triethoxysilane groups with silanol groups on the Si surface, to generate surface bound amine groups. After which the Si substrates were removed from the glass vials while still hot, allowing excess APTES liquid to evaporate, rinsed with toluene, and blown dry with a stream of N_2 gas. The APTES-modified Si substrates were then functionalized with the ATRP initiator BiBB by immersion in a 0.1 M solution of BiBB in toluene, overnight. Finally, they were rinsed with toluene, dried, and immediately used in the following experiments in order to avoid contamination.

ARGET-ATRP of Alkyl Methacrylate Polymer Brushes. AA (0.02−100 mg, 0.1−570 μmol) and ethanol (7 mL) were first mixed in a glass vial (20 mL, 2 cm diameter). $CuCl_2$ (28 mg, 210 μmol) and PMDETA (100 μL, 480 μmol) were mixed in ethanol (10 mL) and allowed to dissolve. A volume of 1 mL of this Cu catalyst solution was then added to the glass vial containing AA and stirred to mix. Monomer (8 mL) was then added to the vial and briefly stirred to mix. After which an initiator substrate was inserted to the reaction solution (polished side upward at the base of the vial) and the glass vial sealed with a screw-top lid. Reaction solutions were not degassed, and glass vials contained ∼4 mL of ambient air. Polymerizations were allowed to proceed at room temperature (23−28 °C) without stirring for the required polymerization time (MMA, 240 min; BuMA and EHMA, 120 min; StMA, 30 min). After polymerization, the substrates were removed from the vial and extensively rinsed with toluene.

Preparation of Perfluorinated Surfaces. A perfluoroalkylsilane monomeric layer was prepared by chemical vapor deposition (CVD) of FAS3 or 17 on UV/ozone-cleaned *n*-type Si (100) wafers, according to our previous report.[38] Each of the substrates was placed, together with a small glass vial containing 0.2 cm^3 of FAS3 or FAS17, into a 60 cm^3 Teflon container in a dry N_2 atmosphere. The container was sealed with a cap and then heated for 72 h at 100 or 150 °C, respectively, in an oven. Samples were then rinsed with *n*-hexane to remove any unreacted material and blown dry with a N_2 stream. The ellipsometrically estimated thicknesses of the adsorbed FAS3 and FAS17 layers on the Si substrates were 0.4 and 0.9 nm, respectively. Judging from the thickness data, the adsorbed FAS3 and FAS17 layers are monomeric with a flat and homogeneous surface (R_{rms} = 0.17 and 0.48 nm, respectively as measured over a 10 × 10 μm^2 area).

Characterization. Polymer brush thickness was determined using spectroscopic ellipsometry (Horiba Jobin-Yvon MM-16) at an incident angle of 70° at wavelengths 500−1000 at 2 nm intervals. Data was modeled using a Cauchy layer with a single Cauchy constant (A = 1.3−1.6 μm). The thicknesses of our polymer brushes as estimated by ellipsometry were 40−60 nm. Contact angles (CAs) were measured using a CA goniometer (Kyowa Interface Science, CA-V150) equipped with a glass sample container filled with the oil under investigation. For measurements of dynamic CAs of water in dichloromethane or dynamic CAs of air bubbles in four organic liquids, a hooked needle and inverted sample holder was used. Briefly, a small drop or bubble was dispensed from the syringe and the volume increased or decreased until the contact line was visibly seen to advance or recede across the surface, respectively, to measure the advancing CA (θ_A) or receding

DOI: 10.1021/acsami.5b02634
ACS Appl. Mater. Interfaces 2015, 7, 12220−12229

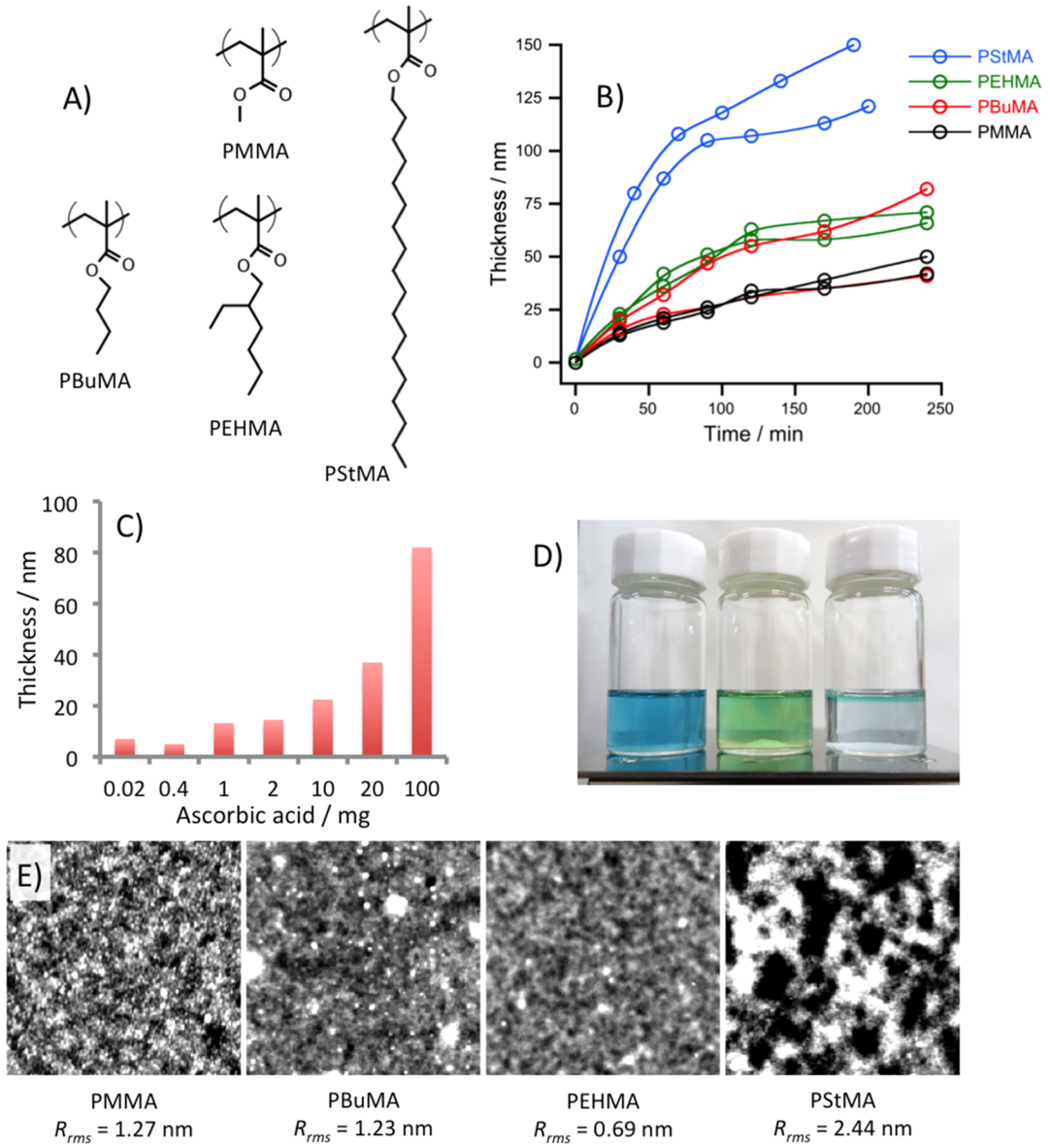

Figure 1. (A) Chemical structures of four polyalkyl methacrylate brushes synthesized in this study. (B) Growth kinetics of the polyalkyl methacrylate brushes using ARGET-ATRP. (C) Effect of the use of different amounts of the reducing agent, ascorbic acid (AA) on the final thickness of polymer brushes (PBuMA). (D) Changes in colors of reaction solutions before and after addition of AA (left, no addition of AA; middle, AA added after monomer addition; right, AA added before monomer addition. (E) AFM images of polymer brush surfaces with R_{rms}. The *z*-scale is +3 nm white, −3 nm black for all images.

CA (θ_R). This process was repeated at least 4 times at 3 different locations on the sample surface. We performed atomic force microscopy (AFM) with a XE-100 microscope (Park Systems, Korea) with a Si probe (Park Systems 910M-NCHR) in tapping mode to study the surface morphology of dry brush surfaces. Before analyzing polymer brush surfaces, all samples were briefly rinsed with toluene (~10 mL) to remove unattached polymer. In our present case, we did not observe any polymerization within reaction solutions.

RESULTS AND DISCUSSION

A range of polyalkyl methacrylate brushes (Figure 1A) were synthesized using ARGET-ATRP. Particular effort was made to produce the brush surfaces under ambient conditions to increase the practical applicability of the developed surfaces, i.e. room temperature and without purging the reaction solution of oxygen. Previously we have reported that water-soluble polymer brushes can be easily produced under such synthetic conditions,[19,21] but as we will show, water-insoluble monomers are less facile to polymerize.

Initially, we tried a variety of solvents and reducing agents in an attempt to find the best preparation method (see Supporting Information, Table S1). Toluene was found to be a good solvent for all of the polymers, monomers, and catalyst complex and was used in combination with the reducing agent tin(II) ethylhexanoate. This combination gave unpredictable results, sometimes polymer brushes grew and other times no polymerization occurred at all. This unpredictability is due to the presence of oxygen in the reaction solution consuming the reducing agent at the start of the polymerization, leaving none to generate Cu(I) from Cu(II). Although, better results were obtained by purging the headspace in the reaction vial with N_2 gas to remove oxygen, this makes the reaction less facile. Using a different reducing agent, ascorbic acid (AA) in toluene, gave a

DOI: 10.1021/acsami.5b02634
ACS Appl. Mater. Interfaces 2015, 7, 12220−12229

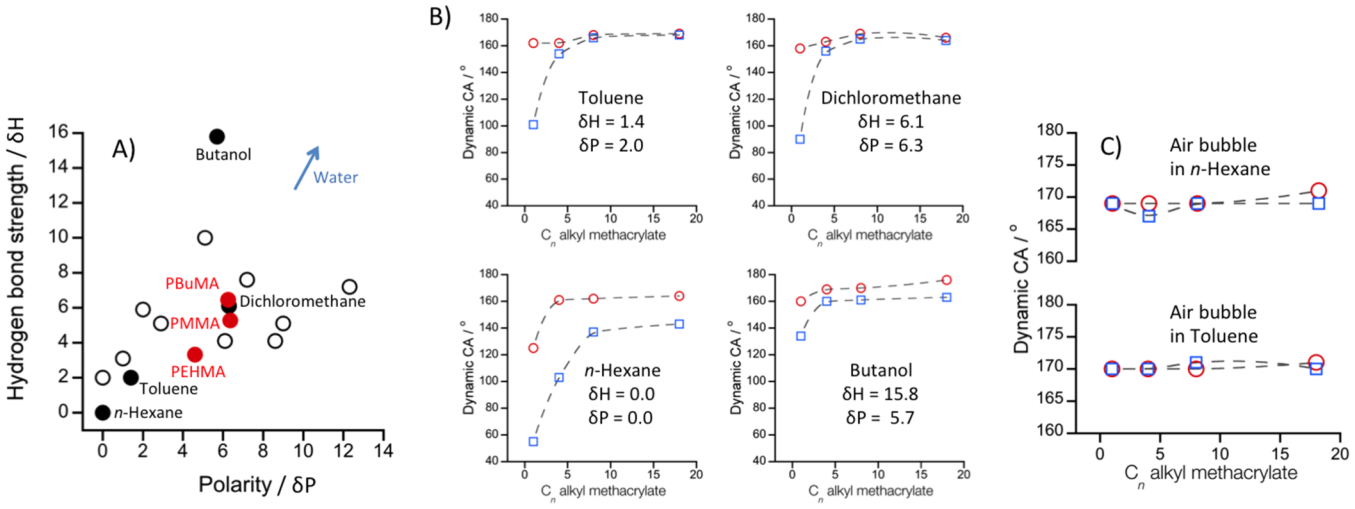

Figure 2. (A) Hansen parameters of several common liquids (unfilled circles), four organic liquids used in this study (filled circles), and three polyalkyl methacrylates (red-filled circles). No data were available for PStMA. (B) θ_A (red-open circles) and θ_R (blue-open squares) of water or (C) air bubbles on polyalkyl methacrylate brushes submerged in different organic liquids.

heterogeneous reaction in which AA did not dissolve. Over the course of several hours, the white powder of AA turned blue indicating that the Cu complex was being adsorbed onto the surface. Under these conditions, only very thin polymer brushes were obtained.

It has been reported that the rate of ATRP is significantly increased in polar solvents such as water and DMF.[39] DMF is also a good solvent for the catalyst, monomers, and all polymers except PStMA. Unfortunately, reactions using DMF did not produce polymer brushes with acceptable thicknesses, (<10 nm) except for PStMA, which produced very thick brushes (321 nm). Finally, we found that the best combination of solvent and reducing agent to use was ethanol with 50% monomer as the solvent and AA as the reducing agent. This combination gave the best polymer brush thicknesses for all alkyl methacrylates investigated.

Figure 1B shows the growth kinetics of polymer brushes prepared using these ethanolic protocols. As can be seen, the thickness after a few hours polymerization time (30−240 min) depended on the alkyl-chain length of the monomer; PMMA gave the smallest thickness, while PStMA gave the thickest. The curvature of plots also seems to depend on the alkyl-chain length with PMMA giving the most linear relationship with the reaction time, while PStMA is the most curved. These growth kinetics suggest that the reactivity of the monomers decreases in the order of StMA > EHMA > BuMA > MMA for our particular system. Overall, StMA polymerization was fast but less controlled (curved plot), while PMMA gave the slowest but most controlled polymerization (linear plot). To achieve nearly identical film thickness of polymer brushes (around 50 nm), MMA, BuMA/EHMA, and StMA were polymerized for 240, 30, and 20 min, respectively.

Next, we investigated how the amount of AA affected the final polymer brush thickness using BuMA. When a small amount of AA was added (0−1 mg), only very thin polymer brushes were obtained (<10 nm), even if the reactions were left to polymerize overnight (Figure 1C). Using larger amounts of AA (>1 mg), the film thickness increased with an increase in the amount of AA, giving a maximum thickness of 82 nm when 100 mg of AA was added to the precursor solutions. However, when more than 10 mg AA was added, not all AA dissolved because of the limited solubility of AA in the monomer/ethanol mixtures.

These results can be explained by observing the color of reaction solutions before and during the reactions as shown in Figure 1D. The Cu(II) complex dissolved in the reaction solution gave a blue color (Figure 1D left), which changes to colorless when AA reduces the catalyst to Cu(I) (Figure 1D right). We observed that when small amounts of AA (<1 mg) were added to the mixture, the color remained blue, highlighting that the majority of catalyst is in the oxidation state (2+). In contrast, when larger amounts of AA (>1 mg) were added, the reaction solution color changed to colorless indicating that the majority of catalyst is in the oxidation state (1+). Depending on the amount of AA present, the reaction solution returned back to blue after a certain amount of time. This time was longest when the highest amounts of AA were used (100 mg). These color changes indicate that unlike in the A(R)GET-ATRP of water-soluble monomers previously reported,[19] hydrophobic monomers cannot polymerize at very low Cu(I)/Cu(II) ratios, but instead require very high ratios. When only small amounts of AA were added to the reaction, this high ratio was either not achieved or only maintained for a small amount of time before residual oxygen oxidized Cu(I) to Cu(II), lowering the ratio and ceasing polymerization. Whereas when large amounts of AA were added, this high ratio could be maintained for longer periods of time yielding more polymerization and thicker polymer brushes.

Crucially, we also found that the order in which the reagents are combined gives markedly different final brush thicknesses. If AA was added to the reaction mixture after monomer, the color remained blue or changed to green/blue (Figure 1D middle). Whereas if ethanol, AA, and catalyst were combined first, then the monomer added and the solution became transparent (Figure 1D right). This order dependency is due to the solubility of AA, which is much higher in ethanol than in ethanol/monomer mixtures. It also highlights that the majority of Cu(I) is probably generated before monomer is added to the reaction and that the ratio of Cu(I)/Cu(II) falls throughout the reaction due to the oxidation by residual oxygen molecules in the solutions.

DOI: 10.1021/acsami.5b02634
ACS Appl. Mater. Interfaces 2015, 7, 12220−12229

Using this protocol, a range of polymer brushes were prepared. AFM confirmed that the obtained polymer brushes gave a homogeneous coverage over the entire Si substrate and that the surfaces were relatively smooth (Figure 1E). The average root-mean-squared roughness (R_{rms}) of the samples was less than 3 nm from the AFM images (10 × 10 μm^2). Although PStMA-covered surfaces seem to be slightly rougher than other polymer surfaces, they are still smooth (R_{rms} = 2.44 nm). This slight increase in surface roughness was probably due to crystallization of the stearyl side chains. We expect that in all cases that the brush surface is even smoother when they are solvated by organic liquids, and thus surface morphology has little if any influence on the wettability differences of sample surfaces.

Next, we investigated the dynamic dewetting properties of our polymer brush surfaces toward water when submerged in various organic liquids. As shown in Figure 2A, common organic liquids have a range of molecular interactions which can be quantified using the Hansen solubility parameters.[40] For this study, we selected four organic liquids (*n*-hexane, toluene, dichloromethane, and 1-butanol) with different physicochemical properties to investigate interactions between these liquids and brush surfaces. *n*-Hexane forms very weak hydrogen bonds and is very nonpolar (δH = 0, δP = 0), toluene forms weak hydrogen bonds and is nonpolar (δH = 1.2, δP = 1.4), dichloromethane possesses moderate hydrogen bond strength and polarity (δH = 6.1, δP = 6.3), whereas 1-butanol forms strong hydrogen bonds but is only moderately polar (δH = 15.8, δP = 5.7). Many liquids relevant to real-life applications have intermolecular interactions similar to these four organic liquids. For example, crude oils (δP ∼ 4, δH ∼ 3) and bitumens (δP ∼ 5, δH ∼ 3)[40] lie between toluene and dichloromethane, Jet fuel JP-5 (δP = 0.2, δH = 0.5)[41] lies between *n*-hexane and toluene, and biodiesels (δH ∼ 7, δP ∼ 5)[42] are similar to dichloromethane. Thus, using these four organic liquids, the dewettability of polymer brushes in conditions equivalent to most industrial applications can be studied.

The θ_A/θ_R values of water drops and CA hysteresis on polyalkyl methacrylate brush surfaces submerged in four organic liquids are shown in Figure 2B and Table 1, respectively. As can be seen, various combinations of organic liquids and polyalkyl methacrylate brushes gave good dynamic hydrophobicity. As discussed in the Introduction section, it is desirable to have either high CAs to minimize the contact area between surfaces and drops and/or negligible CAH to enable drops to slide across surfaces. For example, PStMA (C_n = 18) submerged in toluene showed high dynamic CAs (θ_A/θ_R = 169°/168°) with very low CA hysteresis ($\Delta\theta$ = 1°). Whereas other combinations gave inferior dynamic hydrophobicity, such as PMMA (C_n = 1) in *n*-hexane, which displayed a low θ_A and even lower θ_R (θ_A/θ_R = 125°/55°), giving significant large CA hysteresis ($\Delta\theta$ = 55°). Several trends in the data are apparent. First, the length of the alkyl side chain had a large effect on dynamic CAs, and submerged in any liquids, long-chain polyalkyl methacrylates gave the highest θ_A and θ_R values and the least CA hysteresis. Although, the longest alkyl chain (PStMA, C_n = 18) does not always give significantly better wetting properties than shorter alkyl chains (PEHMA C_n = 8 or PBuMA C_n = 4). In contrast to such similar dewetting behavior, the shortest alkyl chain brush surface (PMMA, C_n = 1) consistently gave poor dynamic dewetting properties, suffering from low θ_R and large CA hysteresis.

Table 1. Measured CA Hysteresis for Each Different Polyalkylmethacrylate Surface Submerged in Different Organic Liquids[a]

Organic Liquid	Polymer			
	PMMA	PBuMA	PEHMA	PStMA
1-butanol	26°	9°	10°	13°
Dichloromethane	68°	7°	4°	2°
Toluene	61°	8°	2°	1°
n-Hexane	70°	58°	25°	21°

[a]Green or red colored numbers indicated that the polymer is soluble or insoluble in the organic liquids, respectively.

Besides the effects of alkyl chain length, we found that CA hysteresis was also influenced by the solubility of the polymer brush in the organic liquids. As shown in Table1, reading across rows shows trends due to solubility of the polymer chain. For example, in 1-butanol or *n*-hexane, lower CA hysteresis was measured when the polymer was soluble in the organic liquid. This can be explained by the solvated polymer chains having higher segmental mobility than unsolvated chains. However, comparing rows in the table seems to contradict this hypothesis. For example, PMMA is insoluble in 1-butanol but has lower CA hysteresis ($\Delta\theta$ = 26°) than in dichloromethane where the polymer is soluble ($\Delta\theta$ = 68°). As can be seen for dichloromethane and toluene, in which all of the polymers are soluble, PMMA has high CA hysteresis ($\Delta\theta$ = 68° and 61°, respectively) giving poor dynamic dewettability, while PStMA has excellent dewettability with very low CA hysteresis ($\Delta\theta$ = 2° in dichloromethane and $\Delta\theta$ = 1° in toluene). Also in *n*-hexane, PEHMA and PStMA are soluble but have moderately high CA hysteresis ($\Delta\theta$ = 25° and 21°, respectively). Therefore, we conclude that solubility of the polymer chain in the organic liquids partially improves dewettability but is secondary to the length of the alkyl chain. Another factor, glass transition temperature (T_g), also does not to seem affect dynamic dewetting behavior when the polymer brush is not solvated. For example, PMMA and PBuMA exhibited large CA hysteresis in *n*-hexane (70° and 58°, respectively), even though the former has T_g above the ambient temperature and the latter below (bulk T_g's of 110 and 20 °C, respectively).

Matching Hansen solubility parameters of the polymer and organic liquids does not seem to result in good dewettability; dichloromethane and PMMA have very similar Hansen solubility parameters (Figure 2A), but there is significant CA hysteresis ($\Delta\theta$ = 68°). PStMA side chains may crystallize when not solvated by an organic liquid (for the case of PStMA in 1-butanol only), but if crystallization occurs, it does not seem to affect the dewetting properties, either positively or negatively. Actually, PStMA's dynamic dewetting behaviors fit with the trends of other noncrystalline polymer brushes.

In addition to water, we also investigated the repellent nature of polyalkyl methacrylate brushes to air bubbles. This is important for practical applications such as hydraulic systems where trapped air bubbles cause lag in response and loss of power.[43] As shown in Figure 2C, submerged in a good solvent like toluene, all polymer brush surfaces were highly repellent toward air bubbles with high dynamic CAs (θ_A/θ_R = 170°/170°) and zero CA hysteresis. In this case, we expect that the

DOI: 10.1021/acsami.5b02634
ACS Appl. Mater. Interfaces 2015, 7, 12220−12229

polymer brush remains swollen by the organic liquid after the surface comes into contact with an air bubble, providing a compressible liquid-like layer with an excellent air-bubble repellent nature. In contrast, when the polymer brush is submerged in a poor solvent such as PMMA or PBuMA in *n*-hexane, it is not solvated and behaves as a hard, rigid layer. However, in both cases, dynamic CAs and CA hysteresis remained almost unchanged as shown in Figure 2C. Thus, we can conclude that air-bubble repellency of the polymer brush is independent of its solvated state. Table 2 summarizes the measured CA hysteresis for our polymer brushes submerged in a good solvent (toluene) or bad solvent (*n*-hexane). In all cases, CA hysteresis was very low ($\Delta\theta$ = 0–2°), highlighting the excellent bubble-repellent nature of polyalkyl methacrylate brushes.

Table 2. CA Hysteresis of Air-Bubbles on Polyalkylmethacrylate Brushes Submerged in *n*-Hexane and Toluene

	Polymer			
Organic Liquid	PMMA	PBuMA	PEHMA	PStMA
Toluene	0°	0°	0°	1°
n-Hexane	0°	2°	0°	2°

We have previously reported that surfaces functionalized with highly branched alkyl chains give superior dynamic dewetting properties compared to linear alkyl chains,[44] and that cis–trans transitions in alkyl chains play an important role in reducing CA hysteresis.[45] With this in mind, we investigated the effects of molecular structure on dynamic hydrophobicity of samples when submerged in the organic liquids using isomers of poly(butyl methacrylate) as shown in Figure 3A. By increasing branching, the number of methyl groups increases, while the number of methylene groups and the chain mobility decrease. As can be seen from Figure 3B, when submerged in *n*-hexane which is a poor solvent, linear-PBuMA and tertiary-PBuMA brush surfaces showed nearly identical dynamic CAs.

Whereas iso-PBuMA brush surface had a receding CA significantly higher than those of two other isomers, resulting in a decrease in CA hysteresis by ~50% ($\Delta\theta$ = 27°). Submerged in toluene, this trend in dewettability markedly changed. Now, linear- and iso-PBuMA brush surfaces exhibited almost identical dynamic CAs, while the tertiary-PBuMA brush surface had a significantly lower receding CA, resulting in a ~3-fold increase in CA hysteresis. Although no prominent trend can be observed in this data, it is clear that branched isomers of PBuMA do not give enhanced dynamic dewetting properties. Substantial improvement in the dewetting properties in *n*-hexane and toluene can be achieved by simply increasing the chain length of alkyl methacrylate rather than by branching.

We also investigated how measured dynamic CAs and CA hysteresis affect the water-repellency of the polyalkyl methacrylate surfaces under real conditions. To do this, we

A)

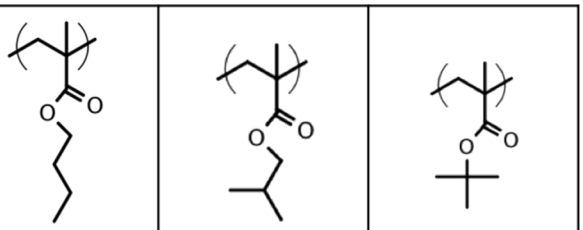

	Linear			Iso			Tertiary		
	θ_A	θ_R	$\Delta\theta$	θ_A	θ_R	$\Delta\theta$	θ_A	θ_R	$\Delta\theta$
In Air	97°	77°	20°	78°	42°	36°	95°	71°	24°
In Toluene	162°	154°	8°	162°	154°	8°	158°	135°	23°
In Hexane	161°	103°	58°	156°	129°	27°	160°	100°	60°

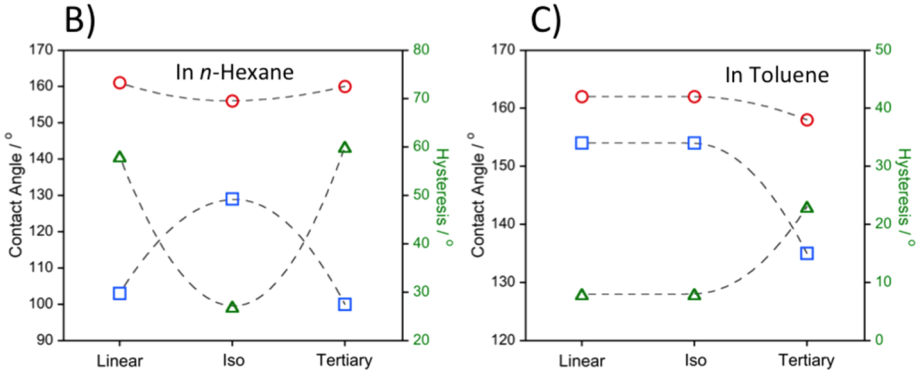

Figure 3. (A) Chemical structures of PBuMA isomers and dynamic water CAs on the resulting surfaces in air, toluene, or *n*-hexane. Dynamic water CAs of PBuMA isomer brush surfaces submerged in (B) *n*-hexane and (C) toluene (θ_A, red-open circles; θ_R, blue-open squares; and CA hysteresis, green-open triangles).

DOI: 10.1021/acsami.5b02634
ACS Appl. Mater. Interfaces 2015, 7, 12220–12229

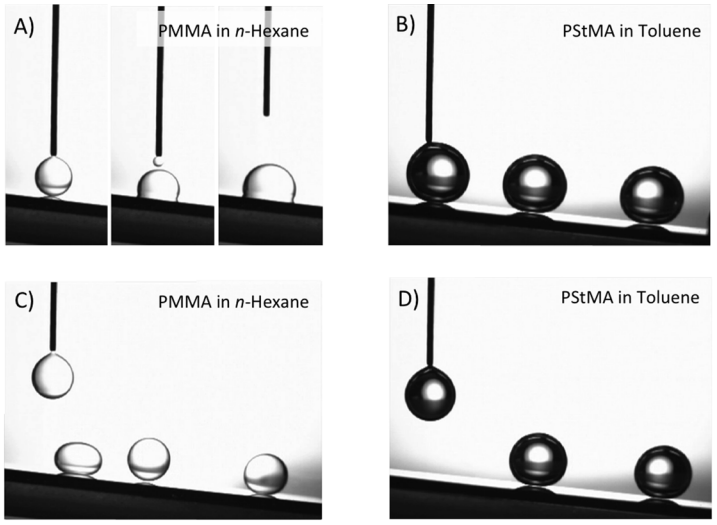

	n-Hexane				Toluene			
	Solubility	ΔCA	Dropped	Placed	Solubility	ΔCA	Dropped	Placed
PMMA	Poor	70°	Slide	Stick	Good	61°	Slide	Stick
PBuMA	Poor	58°	Slide	Stick	Good	8°	Slide	Stick
PEHMA	Good	25°	Slide	Stick	Good	2°	Slide	Slide
PStMA	Good	21°	Slide	Stick	Good	1°	Slide	Slide

Figure 4. Hydrophobicity with moving or static water drops in organic liquids. When water droplets were gently placed onto surfaces they (A) adhered to PMMA in *n*-hexane and (B) slid across PStMA surface in toluene, consistent with measured CA hysteresis (bable below). When dropped from a small height onto the polymer brush surface, they slid across all surfaces: (C) PMMA surface in *n*-hexane, (D) PStMA surfaces in toluene, inconsistent with measured CA hysteresis.

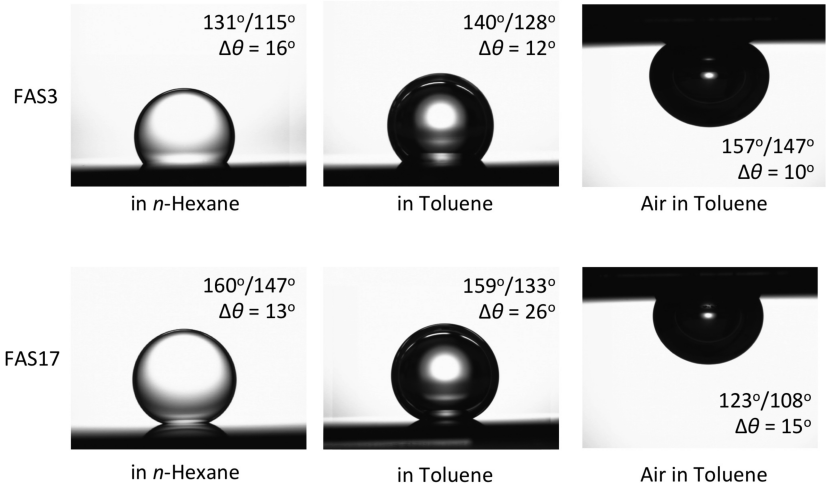

Figure 5. Profiles of water drops and air bubbles formed on conventional perfluoroalkylsilane-monolayer-covered surfaces submerged in toluene or *n*-hexane. θ_A/θ_R and $\Delta\theta$ values for each combination of brush surface and oil are shown in the photographs.

submerged polymer brush surfaces in either a good solvent (toluene) or a poor/nonsolvent (*n*-hexane), inclined the surface to an angle and then observed the motion on water drops on the surfaces (Figure 4). As discussed above, PMMA brush surfaces in *n*-hexane showed high CA hysteresis ($\Delta\theta$ = 70°), which should result in a significant barrier to the mobility of water drops. In contrast, PStMA brush surfaces had negligible CA hysteresis submerged in toluene ($\Delta\theta$ = 1°), meaning that there should not be a significant barrier to water drop mobility. Consistent with these measured dynamic CAs, water drops placed on an inclined PMMA brush surface in *n*-hexane were immobilized and did not slide down the surface (Figure 4A) and drops placed on PStMA brush surfaces in toluene easy slid down the surface (Figure 4B). Overall as shown in the table of Figure 4, water drops were pinned to the surface when moderate to large CA hysteresis was measured

DOI: 10.1021/acsami.5b02634
ACS Appl. Mater. Interfaces 2015, 7, 12220−12229

($\Delta\theta$ = 8−70°) and mobile only when the measured CA hysteresis was negligible ($\Delta\theta$ = 1° or 2°). Again, solubility of the polymers in the organic liquids was not the dominant factor that determines water-repellency and the results are consistent with measured CA hysteresis from captive drop CA measurements.

Different dewetting behavior was observed when water drops impacted onto the surface, rather than being gently placed, even at low impact velocities. As shown in Figure 4C, when water drops (∼3 mm diameter) were dropped from a small height (∼10 mm) and impacted onto a PMMA brush surface under *n*-hexane, they rebounded off the surface and moved across the surface in a series of bounces and slides. After the initial compression of the impact, water drops formed a perfect sphere and appeared to not wet the brush surface at all. This is completely inconsistent with dynamic CA data shown in Figure 2B and Table 1, which measured a significant CA hysteresis ($\Delta\theta$ = 70°). In fact, when water drops impacted onto any of the polyalkyl methacrylate surfaces under any organic liquids, the water drop was always repelled from the surface. Such rebound phenomena has been normally observed only when drops impact onto surfaces at moderately high impact velocities, characterized by Weber numbers of ∼>25.[46,47] However, in Figure 4, the Weber number is calculated to be very small ∼0.1. Even at such a small Weber number, all brush surfaces exhibited similar dynamic dewetting behavior, independent of measured CA hysteresis values. In contrast, only PEHMA and PStMA brush surfaces with negligible CA hysteresis ($\Delta\theta$ = 1−2°) allow water drops to slide across the surface once they become stationary.

As we have shown in the previous section, polyalkyl methacrylate brushes have excellent water and air-bubble repellent natures. In this section we compare polyalkyl methacrylate brush surfaces to conventional perfluorinated surfaces, which are conventionally thought to be nonfouling liquid-repellent surfaces. Figure 5 shows typical water droplet and air bubble profiles on two representative perfluorinated surfaces prepared with short (FAS3) and long-chain (FAS17) perfluoroalkylsilane monolayers. When submerged in either *n*-hexane or toluene, both perfluorinated surfaces showed lower CAs and more CA hysteresis than PStMA in identical conditions. The longer FAS17-monolayer-covered surface showed higher dynamic CAs than the FAS3-monolayer-covered surface, but still suffered from large CA hysteresis ($\Delta\theta$ = 13° and 26°, respectively). In contrast to water repellency, dynamic CAs of air bubbles on the FAS3-monolayer-covered surface (θ_A/θ_R = 157°/147°) were higher than those of FAS17-monolayer-covered surface (θ_A/θ_R = 123°/108°) and both surfaces exhibited nearly identical CA hysteresis ($\Delta\theta$ = 10° and 15°, respectively).

Comparing absolute magnitude of dynamic CAs and CA hysteresis of these perfluoroalkylsilane-monolayer-covered surfaces to long-chain polyalkyl methacrylate (PEHMA and PStMA) brush surfaces, the perfluorinated surfaces have lower CAs and more CA hysteresis. Long-chain perfluorinated surfaces have better hydrophobicity compared to short-chain perfluorinated surfaces but worse air-bubble repellency. These superior properties of our polyalkyl methacrylate brushes originate from the strong molecular interactions between the organic liquids (either toluene or *n*-hexane) and the polymer brushes and relatively weak interactions between water and the polymer brushes. The relative strengths of these interactions ensures that the polymer brush surface is selectively wetted by the organic liquids over water and not dewetted by air bubbles, resulting in large dynamic CAs and low CA hysteresis. Conversely, perfluorinated surfaces possess low surfaces energies, have weak molecular interactions with both organic liquids and water, and exhibit poor selectivity toward being wet by the organic liquids. This nonselectivity results in smaller CAs and larger CA hysteresis, with both water drops and air-bubbles, when submerged in organic liquids.

CONCLUSIONS

Our experimental results offer clear proof that polyalkyl methacrylate brush surfaces give excellent superhydrophobic and air-bubble repellant when submerged in various organic liquids. In addition, neither surface texturing nor perfluorination is required to achieve such surface properties. Preparation by ARGET-ATRP gives simple and facile functionalization and does not require the reaction solution to be purged of oxygen or heated to elevated reaction temperatures. Length of alkyl methacrylate side chain (C_n, where n = 1, 4, 8, and 18) was found to be the most important factor in obtaining superhydrophobic surfaces when submerged in organic liquids. Longer alkyl-chained polymers such as PEHMA (C_8) and PStMA (C_{18}) gave the largest CAs and lowest CA hysteresis with water when submerged in any of the organic liquids. Relatively short-chained polymers such as PBuMA (C_4) could give moderately good superhydrophobicity in certain liquids, but the shortest alkyl chain (PMMA, C_1) always gave poor dewetting properties. Such dewetting properties sometimes improved when polymer chains were solvated by the organic liquids, but this variable was still dominated by the length of alkyl side chain. Branching of the alkyl side chain did yield improvements in dewettability submerged in certain specific organic liquids, but overall dewetting properties were very similar to the linear polyalkyl methacrylates. Under real-life conditions where water drops impact onto the surface at moderate velocities, we found that dynamic hydrophobicity markedly changed. Under these conditions, all polymer brush surfaces were highly water repellent, even when large CA hysteresis was measured using captive drop measurements.

Finally, compared to conventional perfluoroalkylsilane-monolayer-covered surfaces, our polymer brush surfaces displayed superior water and bubble-repellant properties under any organic liquid. We hope that these types of polymer brushes will lead to new functional coatings, for use in a wide range of practical applications, which do not rely on surface roughening or perfluorination.

ASSOCIATED CONTENT

Supporting Information

Results of ARGET-ATRP synthesis of polyalkyl methacrylate brushes using different solvents, reducing agents, and experimental conditions. The Supporting Information is available free of charge on the ACS Publications website at DOI: 10.1021/acsami.5b02634.

AUTHOR INFORMATION

Corresponding Author

*E-mail: a.hozumi@aist.go.jp.

Notes

The authors declare no competing financial interest.

DOI: 10.1021/acsami.5b02634
ACS Appl. Mater. Interfaces 2015, 7, 12220−12229

■ ACKNOWLEDGMENTS

This work was partially supported by a Grant-in-Aid for Scientific Research on Innovative Areas (A.H. and C.U.; Grant No. 24120005) of The Ministry of Education, Culture, Sports, Science, and Technology (MEXT), Japan.

■ REFERENCES

(1) Wang, W.; Jenkins, P. E.; Ren, Z. Heterogeneous Corrosion Behaviour of Carbon Steel in Water Contaminated Biodiesel. *Corros. Sci.* **2011**, *53*, 845−849.
(2) Norouzi, S.; Hazeri, K.; Wyszynski, M. L.; Tsolakis, A. Investigation on the Effects of Temperature, Dissolved Oxygen and Water on Corrosion Behaviour of Aluminium and Copper Exposed to Diesel-Type Liquid Fuels. *Fuel Process. Technol.* **2014**, *128*, 220−231.
(3) Wang, Y.; Li, X.; Li, M.; Shi, B.; Liu, Y.; Mao, L. Preparation of Silica Nanoparticles Catalysed by Small Organic Tertiary Amine and Applications in Surface Coating with Antireflective/Antifogging Properties. *J. Sol−Gel Sci. Technol.* **2014**, *70*, 1−5.
(4) Nuraje, N.; Asmatulu, R.; Cohen, R. E.; Rubner, M. F. Durable Antifog Films from Layer-by-Layer Molecularly Blended Hydrophilic Polysaccharides. *Langmuir* **2011**, *27*, 782−791.
(5) Zhao, Q.; Liu, Y. Investigation of Graded Ni-Cu-P-PTFE Composite Coatings with Antiscaling Properties. *Appl. Surf. Sci.* **2004**, *229*, 56−62.
(6) *Report on the Accident to Boeing 777-236ER, G-YMMM*, at London Heathrow Airport, U.K. on January 17, 2008, Branch, A. A. I., Ed.; 2010.
(7) Li, X.-M.; Reinhoudt, D.; Crego-Calama, M. What Do We Need for a Superhydrophobic Surface? A Review on the Recent Progress in the Preparation of Superhydrophobic Surfaces. *Chem. Soc. Rev.* **2007**, *36*, 1350−1368.
(8) Martin, J. W.; Mabury, S. A.; Solomon, K. R.; Muir, D. C. G. Bioconcentration and Tissue Distribution of Perfluorinated Acids in Rainbow Trout (Oncorhynchus Mykiss). *Environ. Toxicol. Chem.* **2003**, *22*, 196−204.
(9) Martin, J. W.; Whittle, D. M.; Muir, D. C. G.; Mabury, S. A. Perfluoroalkyl Contaminants in a Food Web from Lake Ontario. *Environ. Sci. Technol.* **2004**, *38*, 5379−5385.
(10) In 2013 Gore-Tex eliminated the use of Perfluorooctanoic acid. See http://news.gorefabrics.com/en_gb/enterprise/innovation/gore-completes-elimination-of-pfoa-from-raw-material-of-its-functional-fabrics/ (retreived February 2015).
(11) Miranda, D. F.; Urata, C.; Masheder, B.; Dunderdale, G. J.; Yagihashi, M.; Hozumi, A. Physically and Chemically Stable Ionic Liquid-Infused Textured Surfaces Showing Excellent Dynamic Omniphobicity. *APL Mater.* **2014**, *2*, 056108.
(12) Urata, C.; Masheder, B.; Cheng, D. F.; Hozumi, A. Unusual Dynamic Dewetting Behavior of Smooth Perfluorinated Hybrid Films: Potential Advantages over Conventional Textured and Liquid-Infused Perfluorinated Surfaces. *Langmuir* **2013**, *29*, 12472−12482.
(13) Liu, M.; Wang, S.; Wei, Z.; Song, Y.; Jiang, L. Bioinspired Design of a Superoleophobic and Low Adhesive Water/Solid Interface. *Adv. Mater.* **2009**, *21*, 665−669.
(14) Kobayashi, M.; Terayama, Y.; Yamaguchi, H.; Terada, M.; Murakami, D.; Ishihara, K.; Takahara, A. Wettability and Antifouling Behavior on the Surfaces of Superhydrophilic Polymer Brushes. *Langmuir* **2012**, *28*, 7212−7222.
(15) Lin, L.; Liu, M.; Chen, L.; Chen, P.; Ma, J.; Han, D.; Jiang, L. Bio-Inspired Hierarchical Macromolecule-Nanoclay Hydrogels for Robust Underwater Superoleophobicity. *Adv. Mater.* **2010**, *22*, 4826−30.
(16) Xu, L.-P.; Peng, J.; Liu, Y.; Wen, Y.; Zhang, X.; Jiang, L.; Wang, S. Nacre-Inspired Design of Mechanical Stable Coating with Underwater Superoleophobicity. *ACS Nano* **2013**, *7*, 5077−5083.
(17) Zhang, G.; Zhang, X.; Huang, Y.; Su, Z. A Surface Exhibiting Superoleophobicity Both in Air and in Seawater. *ACS Appl. Mater. Interfaces* **2013**, *5*, 6400−6403.
(18) Xu, L.-P.; Zhao, J.; Su, B.; Liu, X.; Peng, J.; Liu, Y.; Liu, H.; Yang, G.; Jiang, L.; Wen, Y.; Zhang, X.; Wang, S. An Ion-Induced Low-Oil-Adhesion Organic/Inorganic Hybrid Film for Stable Superoleophobicity in Seawater. *Adv. Mater.* **2013**, *25*, 606−611.
(19) Dunderdale, G. J.; Urata, C.; Miranda, D. F.; Hozumi, A.; Large-Scale. and Environmentally-Friendly Synthesis of pH-Responsive Oil-Repellent Polymer Brush Surfaces under Ambient Conditions. *ACS Appl. Mater. Interfaces* **2014**, *6*, 11864−11868.
(20) Dunderdale, G.; Howse, J.; Fairclough, P. pH-Dependent Control of Particle Motion through Surface Interactions with Patterned Polymer Brush Surfaces. *Langmuir* **2012**, *28*, 12955−12961.
(21) Dunderdale, G. J.; Urata, C.; Hozumi, A. An Underwater Superoleophobic Surface That Can Be Activated/Deactivated Via External Triggers. *Langmuir* **2014**, *30*, 13438−13446.
(22) Edmondson, S.; Osborne, V. L.; Huck, W. T. S. Polymer Brushes Via Surface-Initiated Polymerizations. *Chem. Soc. Rev.* **2004**, *33*, 14−22.
(23) Liu, F.; Urban, M. W. Recent Advances and Challenges in Designing Stimuli-Responsive Polymers. *Prog. Polym. Sci.* **2010**, *35*, 3−23.
(24) Stuart, M. A. C.; Huck, W. T. S.; Genzer, J.; Mueller, M.; Ober, C.; Stamm, M.; Sukhorukov, G. B.; Szleifer, I.; Tsukruk, V. V.; Urban, M.; Winnik, F.; Zauscher, S.; Luzinov, I.; Minko, S. Emerging Applications of Stimuli-Responsive Polymer Materials. *Nat. Mater.* **2010**, *9*, 101−113.
(25) Barbey, R.; Lavanant, L.; Paripovic, D.; Schuewer, N.; Sugnaux, C.; Tugulu, S.; Klok, H.-A. Polymer Brushes Via Surface-Initiated Controlled Radical Polymerization: Synthesis, Characterization, Properties, and Applications. *Chem. Rev.* **2009**, *109*, 5437−5527.
(26) Kobayashi, M.; Terada, M.; Takahara, A. Polyelectrolyte Brushes: A Novel Stable Lubrication System in Aqueous Conditions. *Faraday Discuss.* **2012**, *156*, 403−412.
(27) Kobayashi, M.; Terayama, Y.; Hosaka, N.; Kaido, M.; Suzuki, A.; Yamada, N.; Torikai, N.; Ishihara, K.; Takahara, A. Friction Behavior of High-Density Poly(2-Methacryloyloxyethyl Phosphorylcholine) Brush in Aqueous Media. *Soft Matter* **2007**, *3*, 740−746.
(28) Bielecki, R. M.; Crobu, M.; Spencer, N. D. Polymer-Brush Lubrication in Oil: Sliding Beyond the Stribeck Curve. *Tribol. Lett.* **2013**, *49*, 263−272.
(29) Bielecki, R. M.; Benetti, E. M.; Kumar, D.; Spencer, N. D. Lubrication with Oil-Compatible Polymer Brushes. *Tribol. Lett.* **2012**, *45*, 477−487.
(30) Lu, G.; Li, Y.-M.; Lu, C.-H.; Xu, Z.-Z. Corrosion Protection of Iron Surface Modified by Poly(Methyl Methacrylate) Using Surface-Initiated Atom Transfer Radical Polymerization (Si-ATRP). *Colloid Polym. Sci.* **2010**, *288*, 1445−1455.
(31) Barthelemy, B.; Maheux, S.; Devillers, S.; Kanoufi, F.; Combellas, C.; Delhalle, J.; Mekhalif, Z. Synergistic Effect on Corrosion Resistance of Phynox Substrates Grafted with Surface-Initiated ATRP (Co)Polymerization of 2-Methacryloyloxyethyl Phosphorylcholine (MPC) and 2-Hydroxyethyl Methacrylate (HEMA). *ACS Appl. Mater. Interfaces* **2014**, *6*, 10060−10071.
(32) Wu, Y.; Huang, Y.; Ma, H. A Facile Method for Permanent and Functional Surface Modification of Poly(dimethylsiloxane). *J. Am. Chem. Soc.* **2007**, *129*, 7226−7227.
(33) Bocheng, Z.; Edmondson, S. Polydopamine-Melanin Initiators for Surface-Initiated ATRP. *Polymer* **2011**, *52*, 2141−2149.
(34) Edmondson, S.; Armes, S. P. Synthesis of Surface-Initiated Polymer Brushes Using Macro-Initiators. *Polym. Int.* **2009**, *58*, 307−316.
(35) Sweat, D. P.; Kim, M.; Yu, X.; Gopalan, P. A Single-Component Inimer Containing Cross-Linkable Ultrathin Polymer Coating for Dense Polymer Brush Growth. *Langmuir* **2013**, *29*, 3805−3812.
(36) Nicolay, R.; Kwak, Y.; Matyjaszewski, K. A Green Route to Well-Defined High-Molecular-Weight (Co)Polymers Using ARGET ATRP with Alkyl Pseudohalides and Copper Catalysis. *Angew. Chem., Int. Ed.* **2010**, *49*, 541−544.
(37) Zang, D.; Wu, C.; Zhu, R.; Zhang, W.; Yu, X.; Zhang, Y. Porous Copper Surfaces with Improved Superhydrophobicity under Oil and

DOI: 10.1021/acsami.5b02634
ACS Appl. Mater. Interfaces 2015, 7, 12220−12229

Their Application in Oil Separation and Capture from Water. *Chem. Commun.* **2013**, *49*, 8410−8412.
(38) Hozumi, A.; Ushiyama, K.; Sugimura, H.; Takai, O. Fluoroalkylsilane Monolayers Formed by Chemical Vapor Surface Modification on Hydroxylated Oxide Surfaces. *Langmuir* **1999**, *15*, 7600−7604.
(39) Huang, W. X.; Kim, J. B.; Bruening, M. L.; Baker, G. L. Functionalization of Surfaces by Water-Accelerated Atom-Transfer Radical Polymerization of Hydroxyethyl Methacrylate and Subsequent Derivatization. *Macromolecules* **2002**, *35*, 1175−1179.
(40) Hansen, C. M. *Hansen Solubility Parameters: A User's Handbook*, 2nd ed.; CRC Press: Boca Raton, FL, 2007.
(41) Graham, J. L.; Striebich, R. C.; Myers, K. J.; Minus, D. K.; Harrison, W. E. Swelling of Nitrile Rubber by Selected Aromatics Blended in a Synthetic Jet Fuel. *Energy Fuels* **2006**, *20*, 759−765.
(42) Batista, M. M.; Guirardello, R.; Kraehenbuehl, M. A. Determination of the Solubility Parameters of Biodiesel from Vegetable Oils. *Energy Fuels* **2013**, *27*, 7497−7509.
(43) Durfee, W.; Sun, Z. *Fluid Power System Dynamics*; Centre for Compact and Efficient Fluid Power, University of Minnesota, 2009.
(44) Masheder, B.; Urata, C.; Hozumi, A. Transparent and Hard Zirconia-Based Hybrid Coatings with Excellent Dynamic/Thermoresponsive Oleophobicity, Thermal Durability, and Hydrolytic Stability. *ACS Appl. Mater. Interfaces* **2013**, *5*, 7899−7905.
(45) Urata, C.; Masheder, B.; Cheng, D. F.; Miranda, D. F.; Dunderdale, G. J.; Miyamae, T.; Hozumi, A. Why Can Organic Liquids Move Easily on Smooth Alkyl-Terminated Surfaces? *Langmuir* **2014**, *30*, 4049−4055.
(46) Antonini, C.; Villa, F.; Bernagozzi, I.; Amirfazli, A. Marengo, M. Drop Rebound after Impact: The Role of the Receding Contact Angle. *Langmuir* **2013**, *29*, 16045−16050.
(47) Kim, H.; Lee, C.; Kim, M. H.; Kim, J. Drop Impact Characteristics and Structure Effects of Hydrophobic Surfaces with Micro- and/or Nanoscaled Structures. *Langmuir* **2012**, *28*, 11250−11257.

DOI: 10.1021/acsami.5b02634
ACS Appl. Mater. Interfaces 2015, 7, 12220−12229